Biophotonic tool for sensing the dynamics of H_2O_2 extracellular release in stressed cells

G. Suárez,*[a] Ch. Santschi,[a] S. Dutta-Gupta,[a] L. Juillerat-Jeanneret[b] and O. J. F. Martin[a]

[1]Nanophotonics and Metrology Laboratory, Swiss Federal Institute of Technology Lausanne (EPFL), CH-1015 Lausanne, Switzerland
[2] Institute of Pathology University of Lausanne (IUP), Rue du Bugnon 25, CH-1011 Lausanne, Switzerland

*guillaume.suarez@epfl.ch; phone +41216936871; fax +41216932614; www.nam.epfl.ch

ABSTRACT

Hydrogen peroxide (H_2O_2) is known to play a multifaceted role in cell physiology mechanisms involving oxidative stress and intracellular signal transduction. Therefore, the development of analytical tools providing information on the dynamics of H_2O_2 generation remains of utmost importance to achieve further insight in the complex physiological processes of living cells and their response to environmental stress[1]. In the present work we developed a novel optic biosensor that provides continuous real-time quantification of the dynamics of the hydrogen peroxide release from cells under oxidative stress conditions. The biosensor is based on the ultra-sensitive dark field optical detection of cytochrome *c* (cyt *c*) that exhibits a narrow absorption peaks in its reduced state (Fe(II)) at λ = 550 nm. In the presence of H_2O_2 the ferrous heme group Fe(II) is oxidised into Fe(III) providing the spectroscopic information exploited in this approach. Extremely low limit-of-detection for H_2O_2 down to the subnanomolar range is achieved by combining scattering substrates (eg. polystyrene beads) able to shelter cyt *c* and an inverted microscope in dark field configuration. The developed biosensor was able to perform real-time detection of H_2O_2 extracellular release from human promyelocytic leukemia cells (HL-60) exposed to lipopolysaccaride (LPS) that elicits strong immune-response. This biosensing tool is currently being implemented to the real-time detection of superoxide anion ($O_2^{\cdot-}$) and offers the possibility to extend to further oxidative stress biomarkers such as glutathione. More generally, multianalyte and dynamic informations might bring new insights to understand complex cellular metabolisms involved in oxidative-stress-related diseases and cytotoxic responses.

Keywords: Biosensor, Real-time, Human cell, Oxidative stress, Reactive oxygen species

1. INTRODUCTION

Reactive Oxidative Species (ROS) are key players in chemical and biological and environmental systems. In the biological context, for instance, the most prominent representatives of ROS are the superoxide anion ($O_2^{\cdot-}$), hydroxyl radical (OH), hydrogen peroxide (H_2O_2) and the nitrogen oxide radical (NO). ROS are essential elements ensuring smooth cycling of healthy physiological processes. However, a misled production of ROS may account for cellular damage, genetic mutation, cancer, neurological disorders and the degenerated process of biological aging[2]. The delicate balance between advantageous, which are related to cell signalling and immune response against viruses and bacteria[3], and detrimental effects causing oxidative stress, e.g. lipid peroxidation and modifications in apoptosis, is certainly a crucial aspect of life which underlines the needs for their ultrasensitive detection. Additionally to the key role that H_2O_2 plays within the oxidative stress paradigm and its implication in environmental and medical issues, its detection results particularly useful in many other contexts since H_2O_2 is a by-product of several enzyme-catalysed reactions. Thus, detecting H_2O_2 represents an indirect way to sense a series of analytes, ranging from sugars and phenols to neurotransmitters, via the so-called coupled-enzyme or bi-enzymatic biosensor configurations.

The ability to sense physiological and biological parameters represents a stimulating area in cell biology with strong

Optical Diagnostics and Sensing XII: Toward Point-of-Care Diagnostics; and Design and Performance Validation of Phantoms Used in Conjunction with Optical Measurement of Tissue IV, edited by Robert J. Nordstrom, Gerard L. Coté, Proc. of SPIE Vol. 8229, 822908 · © 2012 SPIE · CCC code: 1605-7422/12/$18 · doi: 10.1117/12.910318

impact on diagnostics and therapies[4,5]. The recent cross-disciplinary integration of nanotechnology, biology and photonics led to the emergence of different nanotools – such as nanoprobes and nanobiosensors – that allow the detection of a series of (bio)chemical targets in individual living cells[6]. Unlike classical biochemical assays carried out with isolated molecules from lysed cells in test tubes, these nanotools enable elucidating intimate life processes occurring at the molecular level. Simple biochemical tests are commercially available that rely on membrane-permeable low molecular weight dyes that react specifically with intracellular targets, giving rise to fluorescence signals development. Such chemical probes allow end-point intracellular detection of a series of biomarkers that provide evidences for key biological mechanisms, such as oxidative stress, lipid peroxidation or cell apoptosis. However, this technique is not fully compatible with a real time monitoring approach and, furthermore, fluorescent dyes might suffer from bleaching for long exposure times. Additionally, long-time exposure to dye may induce cytotoxic effects on analyzed cells. The latter issue has been circumvented with the use of intracellular nanosensors – so called PEBBLE (Probes Encapsulated By Biological Localised Embedding) – that consist in responsive fluorescent dyes encapsulated in porous polyacrylamide nanospheres which are delivered into the intracellular domain of mamalian cells[7,8]. In parallel, many other fluorescent-based probes have been recently studied and developed that take advantage of novel optical and electronic properties of semiconductor quantum dots (QDs). Those spherical nanocrystals with diameters in the order of 2-10 nm are characterized by a bandgap energy that dependents on the particle size. They are significantly brighter and more stable than organic dyes and fluorescent proteins. Numerous applications rely on QDs-assisted Fluorescence Resonance Energy Transfer (FRET) where association/dissociation mechanisms between intracellular biomolecules can be efficiently monitored[9,10].

In such a context, the ability to perform real-time and non-invasive detection of scarce concentrations (i.e. down to sub-nanomolar) of H_2O_2 and, consequently, a variety of other molecules, opens numerous application potentials in domains such as cytotoxicity, environment survey, medical diagnosis or food analysis.

In the present work a novel sensitive and non-invasive detection method for real-time measurement of H_2O_2 has been developed within the perspective of further implementation into a multianalyte detection platform.

2. METHOD FOR REAL-TIME AND SENSITIVE H_2O_2 DETECTION

2.1. Principle and set-up

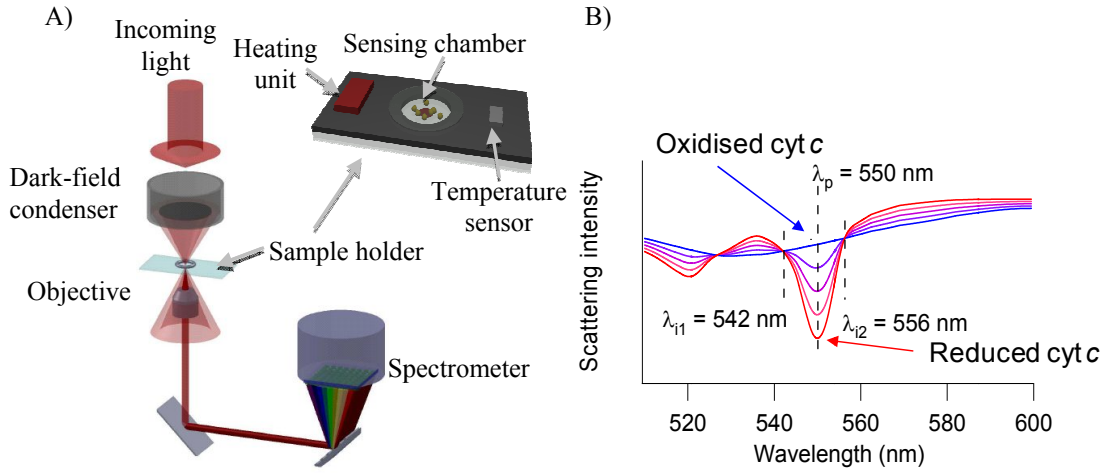

Figure 1. A) Optical set-up including inverted microscope in dark-field configuration with spectrometer and temperature controlled sample holder. B) Optical spectra of cyt *c* recorded from a dark-field set-up showing an absorption peak at λ_p = 550 nm in the reduced state. The degree of strength of the absorption peak varies with the oxidation state and provides an indicator allowing quantification of H_2O_2.

The optical detection of the redox state of hemeproteins (HP), more precisely cytochrome *c* (cyt *c*), represents the core of this method for the sensitive detection of H_2O_2. Depending on its oxidation state cyt *c* exhibits different absorption properties which can be used for the detection, namely, a broad absorption peak at $\lambda = 530$ nm and narrower peaks at $\lambda = 520$ and $\lambda = 550$ nm[11]. The redox catalytic activity of cyt *c*, the pseudo-peroxidase behavior, in which the ferrous Fe^{II} heme group is oxidized into the ferric Fe^{III} heme group leading to H_2O_2 reduction into water, provides the spectroscopic information exploited here. Using an optical set-up in dark-field configuration, the temporal evolution of the oxidation state of cyt *c* is recorded, providing the dynamic measurement of H_2O_2 generation. Figure 1B shows absorption spectra of cyc *c* at different oxidation states. In order to improve the sensitivity of the measurements a porous substrate sheltering cyt *c* is used, leading to an efficient multiscattering – i.e. an increase of the optical trajectory – and therefore an improved detection limit. Moreover, the raw spectral data are converted into a normalized oxidation state coefficient ϕ corresponding to the average oxidation state of the cyt *c* measured in the experiment. The value of ϕ ranges from 0 to 1 for fully oxidized and reduced cyt *c*, respectively and does not dependent on the variation of the signal background.

Environmental changes such as temperature can affect the dynamics of the metabolism of mammalian cells and, hence, lead to a change of ROS production. In order to minimize such a parasitical generation of ROS during the measurements the temperature of the reaction chamber, as depicted in Fig. 1A, is stabilized at 37 °C using a closed loop temperature controller.

2.2. Data treatment

The oxidation state coefficient ϕ provides a value allowing comparison between different experiments. However, a correct comparison requires removing the background signal produced by the microorganisms, the scattering substrate and the liquid medium where the organisms are suspended. The data analysis is based on the superposition of the recorded dark field spectrum with the reference absorption spectrum of cyt *c*[11]. This superposition requires a translation T followed by a shear transformation S and relies on the observation that the intersection points of the oxidized and reduced absorption curves intersect at $\lambda_1 = 542$ nm and $\lambda_2 = 556$ nm. Hence, the scattering intensity at these two wavelengths is independent of the oxidation state of cyt *c*. These two wavelengths provide, therefore, anchor points for the transformation of raw data into the reference spectra, assuming in agreement with the experimental measurements, that the background signal is linear in the interval delimited by λ_1 and λ_2. The following operations are used:

1. Translation T
2. Shear transformation S
3. Scalar multiplication k

$$P_i = kS\left(P'_i - T\right) \tag{1}$$

Applying this operations to $P'(\lambda_1 = 542\text{ nm})$ and $P'(\lambda_2 = 556\text{ nm})$ results in a system of linear independent equations. Finally, the oxidation state coefficient ϕ can be determined from the following definition:

$$\phi = \frac{A_r - A_2}{A_2}, \tag{2}$$

where A_r and A_2 are the absorption at $\lambda_r = 550$ nm and λ_2, respectively. Normalisation of ϕ with respect to the absorption spectra of fully reduced and oxidised cyt *c* provides the ratio of the average cyt *c* oxidation state at a given time of the experiment.

3. ANALYTICAL PERFORMANCES

3.1. Detection of hydrogen peroxide

The analytical performances of the developed biosensor were evaluated via the analysis of a calibration curve. The variation of the oxidation state coefficient, $\Delta\phi$, consecutive to successive additions of known concentrations of H_2O_2

gave rise to the calibration curve shown in Figure 2. The sigmoidal shape of the calibration is typical for ligand binding assay (LBA) that can be fitted with the 4-parameter logistic (4-PL) model[12]. The experiment starts with a partially reduced cyt *c* sample stabilized in HEPES buffer solution, and then the value of ϕ decreases with H_2O_2 concentration over a dynamic range from 10 pM to 1 µM. The calculation of the limit-of-detection (LOD), defined as 3-folds the deviation of the blank, is below 100 pM of H_2O_2 which is, to the best of our knowledge, the lowest LOD ever reported for biosensor tools and at least one order of magnitude lower than values described in the literature[13,14].

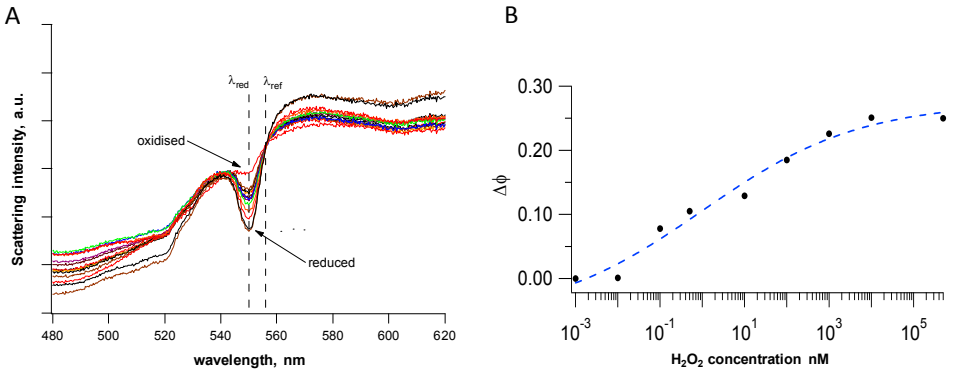

Figure 2. Dependence of the oxidation state coefficient ϕ on H_2O_2 concentration as indicated by A) the evolution of the experimental spectra upon addition of H_2O_2 and B) the typical LBA calibration curve obtained after calculation of ϕ variation.

3.2. Multitarget configuration: detection of superoxide anion

Moreover, the ability of the developed biosensor to detect concentrations of H_2O_2 down to the subnanomolar range paves the way for a multitarget configuration. This implementation is made possible by combining cyt *c* with an enzyme whose catalytic reaction generates H_2O_2 as by-product. This approach has been evaluated for the detection of superoxide anion, $O_2^{\cdot-}$, a representative ROS involved in many metabolic processes such as cell signaling, immunoreactions and oxidative stress. In this experiment $O_2^{\cdot-}$ was enzymatically generated in the sensing chamber as the product of the catalysis of hypoxanthine (HX) by xanthine oxidase (XOD). Then, the highly reactive $O_2^{\cdot-}$ was catalytically converted into H_2O_2 by superoxide dismutase (SOD). Finally, the presence of $O_2^{\cdot-}$ was indirectly detected via the SOD-generation of H_2O_2 that resulted in a decrease of the oxidative coefficient ϕ measured by the biosensor.

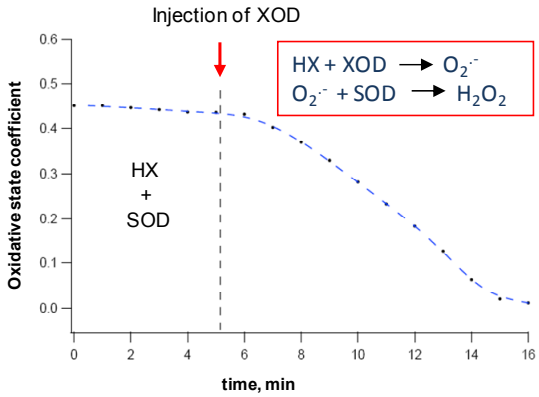

Figure 3. Time-evolution of the oxidation state coefficient ϕ due to real-time production of enzymatic $O_2^{\cdot-}$ once converted into H_2O_2 via SOD catalysis.

4. DYNAMIC DETECTION OF H_2O_2 RELEASED BY HL-60 CELLS

Accessing metabolic mechanisms within living cells holds promising potentials for achieving further discoveries in many health-related domains such as diagnosis, therapy and toxicology. In that context, the ability to detect the dynamics of production/consuption of biomarkers involved in the metabolism of living cells is of major importance. In this study, the applicability of the developed biosensor was put to the test through the real-time detection of H_2O_2 produced by HL-60 cells that constitute a human leukemic cell line. HL-60 cells are particularly adequate model cells to study the mechanism regulating the differentiation along the monocyte/macrophage or granulocytic/neutrophillic lineage[15]. The pyrogenicsensitivity of macrophage-like cells derived from HL-60 differentiation gave rise to the development of several assays for the detection of bacteria, fungi or yeast fragments[16]. However, until recent years it was believed that undifferentiated HL-60 cells have no ability to generate ROS when responding to stimuli. In their pioneer work published in 2005, Muranaka et al. managed to detect via sensitive fluorescent analysis that undifferentiated HL-60 do generate ROS upon stimulation, in a similar way to that of neutrophils[17]. With this in mind, we used our real-time biosensor to evaluate the effect of the bacterial component lipopolysaccharides (LPS) on undifferentiated HL-60 cells.

4.1. Cell culture conditions

HL-60 cells are non-adherent and were grown in suspension. The cells were passaged two times per week in DMEM HG (Gibco®) supplemented with 10% heat-inactivated fetal calf serum in addition to penicillin (100U/ml) and streptomycin (100 ug/ml). Prior to measurements HL-60 cells were pelleted (centrifuge 200xg) and recollected in culture medium without phenol red in order to avoid interferences. After cell counting, 300 µL of cell culture containing 2.10^6 cells mL^{-1} were introduced into the sensing chamber set at 37°C. A stock solution of 1 mg mL^{-1} LPS extracted from *Salmonella typhosa* (Sigma) was prepared in PBS.

4.2. Dynamic detection of H_2O_2 release as HL-60 response to LPS

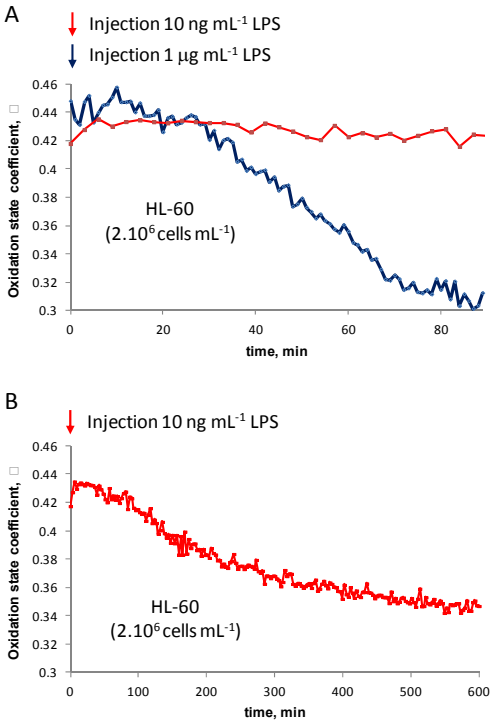

Figure 4. Time-evolution of the oxidation state coefficient ϕ upon real-time release of H_2O_2 produced by HL-60 cells in contact to: A) 1 µg mL^{-1} (blue) and 10 ng mL^{-1} (red) of LPS over a period of 90 min; B) 10 ng mL^{-1} of LPS over a period of 10 hours.

The evolution of the oxidation state coefficient calculated from measured raw spectra provides a clear information on the effect of different concentrations of LPS on HL-60 cells. The blue curve in Fig. 4A indicates that the presence of 1 μg mL^{-1} of LPS in the cell suspension rapidly induces the generation and release of H_2O_2 within approximately 30 min after LPS injection. In comparison, during the first 90 min of the experiment where 10 ng mL^{-1} of LPS is introduced in the sensing chamber almost no extracellular H_2O_2 is registered. For this lower LPS concentration, the release of H_2O_2 appears at t = 90 min and is observable during a period of 10 hours, as shown in Fig. 4B.

5. CONCLUSION

A highly sensitive biophotonic tool was developed that performs real-time detection of H_2O_2 at the subnanomolar level. Dark-field spectroscopy of cyt *c* combined with a substrate exhibiting a high scattering cross-section provides the information on the cyt *c* oxidation state, and, thus, on its oxidation by H_2O_2 molecules. The device was able to sense the dynamics of H_2O_2 extracellular release in human leukemic cells as a response to various concentrations of bacterial components. The implementation of the current biosensor to the real-time detection of further oxidative-stress-related biomarkers might lead to a dynamic toxicity platform able to evaluate the impact of potentially pathogenic organisms and/or materials on cells.

REFERENCES

[1] Maynard, A. D., Aitken, R. J., Butz, T., Colvin, V., Donaldson, K., Oberdorster, G., Philbert, M. A., Ryan, J., Seaton, A., Stone, V., Tinkle, S. S., Tran, L., Walker, N. J. and Warheit, D. B., "Safe handling of nanotechnology," Nature 444(7117), 267-269 (2006).

[2] Harman, D., "The aging process," Proceedings of the National Academy of Sciences of the United States of America-Biological Sciences 78(11), 7124-7128 (1981).

[3] Droge, W., "Free radicals in the physiological control of cell function," Physiological Reviews 82(1), 47-95 (2002).

[4] Ahmad, A. and Moore, E. J., "Comparison of cell-based biosensors with traditional analytical techniques for cytotoxicity monitoring and screening of polycyclic aromatic hydrocarbons in the environment," Analytical Letters 42(1), 1-28 (2009).

[5] Vo-Dinh, T. and Kasili, P., "Fiber-optic nanosensors for single-cell monitoring," Analytical and Bioanalytical Chemistry 382(4), 918-925 (2005).

[6] Zandonella, C., "Cell nanotechnology: The tiny toolkit," Nature 423(6935), 10-12 (2003).

[7] Henderson, J. R., Fulton, D. A., McNeil, C. J. and Manning, P., "The development and in vitro characterisation of an intracellular nanosensor responsive to reactive oxygen species," Biosensors and Bioelectronics 24(12), 3608-3614 (2009).

[8] Webster, A., Coupland, P., Houghton, F. D., Leese, H. J. and Aylott, J. W., "The delivery of PEBBLE nanosensors to measure the intracellular environment," Biochemical Society Transactions 35538-543 (2007).

[9] McGrath, N. and Barroso, M., "Quantum dots as fluorescence resonance energy transfer donors in cells," Journal of Biomedical Optics 13(3), (2008).

[10] Medintz, I. L., "Recent progress in developing FRET-based intracellular sensors for the detection of small molecule nutrients and ligands," Trends in Biotechnology 24(12), 539-542 (2006).

[11] Butt, W. D. and Keilin, D., "Absorption spectra and some other properties of cytochrome *c* and of its compounds with ligands," Proceedings of the Royal Society of London Series B-Biological Sciences 156(965), 429-& (1962).

[12] Findlay, J. W. A. and Dillard, R. F., "Appropriate calibration curve fitting in ligand binding assays," AAPS Journal 9(2), E260-E267 (2007).

[13] Casanova, D., Bouzigues, C., Nguyen, T. L., Ramodiharilafy, R. O., Bouzhir-Sima, L., Gacoin, T., Boilot, J. P., Tharaux, P. L. and Alexandrou, A., "Single europium-doped nanoparticles measure temporal pattern of reactive oxygen species production inside cells," Nat. Nanotechnol. 4(9), 581-585 (2009).

[14] Jin, H., Heller, D. A., Kalbacova, M., Kim, J. H., Zhang, J. Q., Boghossian, A. A., Maheshri, N. and Strano, M. S., "Detection of single-molecule H_2O_2 signalling from epidermal growth factor receptor using fluorescent single-walled carbon nanotubes," Nat. Nanotechnol. 5(4), 302-U381 (2010).

[15] Chatterjee, D., Han, Z. Y., Mendoza, J., Goodglick, L., Hendrickson, E. A., Pantazis, P. and Wyche, J. H., "Monocytic differentiation of HL-60 promyelocytic leukemia cells correlates with the induction of Bcl-x(L)," Cell Growth & Differentiation 8(10), 1083-1089 (1997).

[16] Timm, M., Hansen, E. W., Moesby, L. and Christensen, J. D., "Utilization of the human cell line HL-60 for chemiluminescence based detection of microorganisms and related substances," European Journal of Pharmaceutical Sciences 27(2-3), 252-258 (2006).

[17] Muranaka, S., Fujita, H., Fujiwara, T., Ogino, T., Sato, E. F., Akiyama, J., Imada, I., Inoue, M. and Utsumi, K., "Mechanism and characteristics of stimuli-dependent ROS generation in undifferentiated HL-60 cells," Antioxidants & Redox Signaling 7(9-10), 1367-1376 (2005).